

УДК 538.9

**A. Korneev, M. Finkel, S. Maslennikov, Yu. Korneeva, I. Florya, M. Tarkhov, M. Elezov, S. Ryabchun, I. Tretyakov, A. Isupova, B. Voronov, G. Goltzman**

Moscow State Pedagogical University  
Malaya Pirogovskaya 1, Moscow, 119991, Russia  
E-mail: akorneev@rplab.ru

## **SUPERCONDUCTING NBN TERAHERTZ DETECTORS AND INFRARED PHOTON COUNTERS \***

We present our recent achievements in the development of sensitive and ultrafast thin-film superconducting sensors: hot-electron bolometers (HEB), HEB-mixers for terahertz range and infrared single-photon counters. These sensors have already demonstrated a performance that makes them devices-of-choice for many terahertz and optical applications.

*Keywords:* Hot electron bolometer mixers, infrared single-photon detectors, superconducting device fabrication, superconducting NbN films.

**А. Корнеев, М. Финкель, С. Масленников, Ю. Корнеева, И. Флорья, М. Тархов, М. Елезов, С. Рябчун, И. Третьяков, А. Исупова, Б. Воронов, Г. Гольцман**

### **СВЕРХПРОВОДЯЩИЕ ТЕРАГЕРЦЕВЫЕ NbN ПРИЕМНИКИ И СЧЕТЧИКИ ИК ФОТОНОВ**

Мы представляем свои последние достижения в разработке чувствительных и ультрабыстрых тонкопленочных сверхпроводящих датчиков: болометры на горячих электронах (НЕВ), НЕВ-смесители ТГц диапазона и счетчики одиночных фотонов ИК диапазона. Эти датчики уже продемонстрировали параметры, которые делают их предпочтительными для многих ТГц и оптических приложений.

*Ключевые слова:* смесители и болометры на горячих электронах, счетчики одиночных ИК фотонов, производство сверхпроводящих устройств, сверхпроводящие NbN пленки.

### **Introduction**

The hot-electron effect in thin superconducting films since its discover in early 80's was proposed to develop sensitive bolometers and bolometric mixers for very high frequencies, up to visible region. The bolometers based on hot-electron effect in ultra thin superconducting films (hot-electron bolometer, HEB) demonstrate a unique set of characteristics: very high operation speed ( $\sim 1$  ns for MoRe films,  $\sim 50$  ps for NbN films) and rather good noise equivalent power NEP ( $\sim 10^{-14}$  W\*Hz<sup>-0.5</sup>

for MoRe and Nb,  $\sim 10^{-13}$  W\*Hz<sup>-0.5</sup> for NbN) at temperatures  $\sim 8-10$  K, easily available with commercial closed-cycle cryocoolers. These characteristics are available mainly due to nano-scale dimensions of the sensitive element: the bolometer is a superconducting bridge with  $\sim 0.1 \mu\text{m} \times 1 \mu\text{m}$  in-plane dimensions made from 3-7 nm thick film. For efficient coupling of the bolometer with the radiation it is placed at the feed of either a planar golden log-spiral antenna with multi-octave band (fig. 1), or double-slot antenna with  $\sim 30\%$  band. Bolometers operate at temperatures slightly below

---

\* This work is supported in part by grants of Russian Ministry of Education and Science No 02.740.11.0228, No 2542, and Grant of Russian Federation President No 02.120.11.2221-MK.

critical (superconducting transition temperature,  $T_c$ ), with additional heating of electron subsystem exactly to  $T_c$  with bias current. In this operating regime bolometers provide responsivity of  $\sim 10^4$  and maximum dynamic range for a given volume of active superconducting bridge.

### Hot-electron bolometer mixer characterization

Hot-Electron Bolometer (HEB) mixers have long ago established themselves as the primary detectors of choice for heterodyne observation in terahertz radio astronomy. At the same time, the quest for better characteristics: a lower noise temperature and a wider intermediate frequency (IF) bandwidth has been underway. For a long time the achievement of low noise temperature was hampered by the contact electrical resistance between the antenna and the superconducting bridge of the bolometer. Recently we managed to reduce this resistance significantly by the improvement of the fabrication process. HEB mixers were fabricated from 3.5-nm NbN films deposited on top of Si substrates by DC reactive magnetron sputtering. The deposition of NbN film was followed by in-situ deposition of a 15-nm Au layer. The NbN-Au structure was then covered with electronic resist and a window was made in the resist for the subsequent ion milling and chemical etching of the Au layer all the way down to the NbN film. This defined the bolometer length. The devices had superconducting transition temperatures of about 11.5K with transition

widths of about 1 K. The critical currents were measured to be close to 400  $\mu\text{A}$  and the normal state resistances were 60 to 100 Ohm. When the bolometer is used as a mixer it is operated at temperatures well below  $T_c$  and sufficient local oscillator (LO) power is applied. The best characteristics achieved with NbN HEB mixer are: the noise temperature of several quantum limits ( $hf/k$ , where  $h$  is Planck's constant,  $f$  is the LO frequency,  $k$  – Boltzmann's constant), and a gain bandwidth of 5-6 GHz. At THz frequencies well above 1 THz the NbN HEB mixer outperforms any other mixers operating in this frequency range. Another advantage is rather low LO power required for optimal

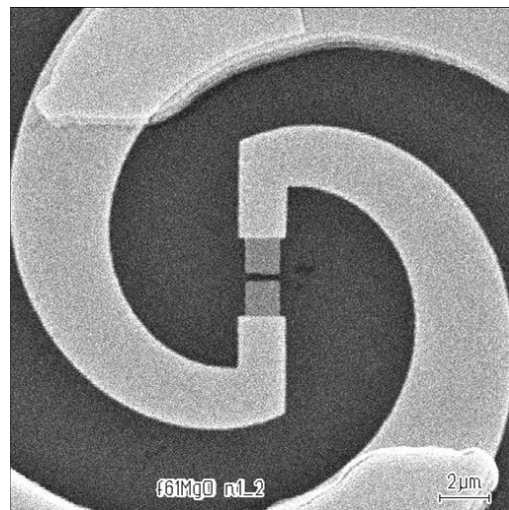


Fig. 1. The scanning electron microscope image of the Hot Electron Bolometer (in the center) integrated with the log-spiral antenna

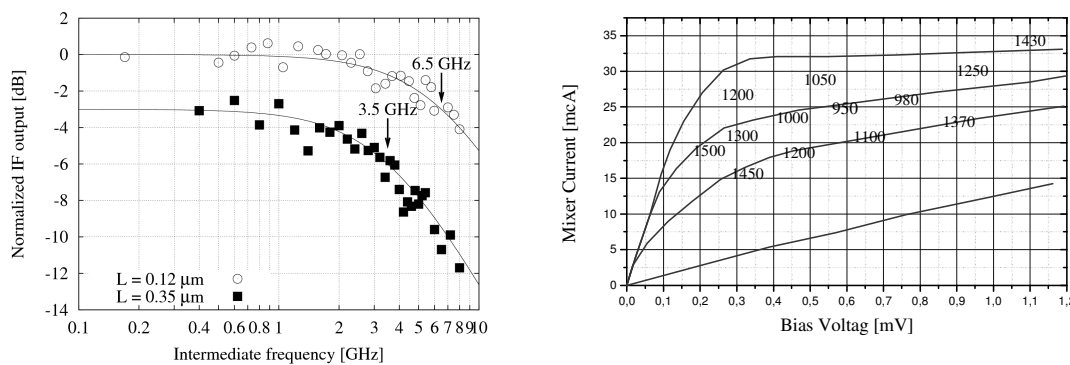


Fig. 2. The dependence of mixer's gain on the intermediate frequency (right); IV-curves family of the single device (left), the figures mark the noise temperatures at the corresponding operation conditions

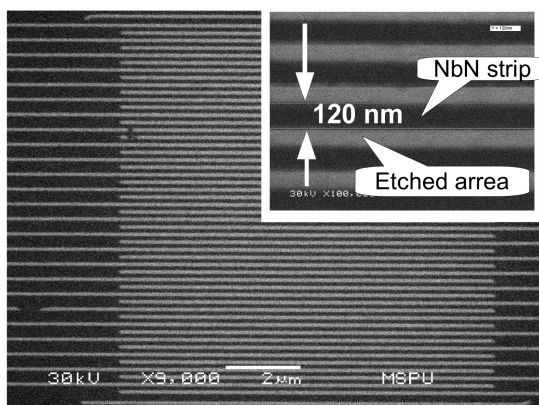


Fig. 3. SEM image of the NbN SSPD: the strip width is 120 nm, the gap between the strips is 80 nm

performance of this mixer (this characteristic depends on mixer element volume,  $\sim 100$  nW has been reported). Figure 2 (left) shows the dependence of mixer's gain on the intermediate frequency whereas figure 2 (right) shows the IV-curves family of the single device with receiver noise temperature in double sideband regime at 2.5 THz LO frequency. The noise temperatures at the corresponding operation conditions (the voltage is controlled with a bias source, the current is mainly controlled with LO power, the more LO power is applied, the lower is mixer's current at the given voltage) are also marked on the figure.

### Superconducting single-photon detector (SSPD) as infrared photon counter for middle infrared

Another promising type of the photon counting detector is superconducting single-photon detector (SSPD) [1]. The SSPD is patterned from 4-nm-thick NbN film as 120-nm-wide and meander-shaped strip that covers a square area of  $10 \mu\text{m} \times 10 \mu\text{m}$  for better coupling with optical radiation (fig. 3). The devices are fabricated using the process based on the direct electron beam lithography and the reactive ion etching [2].

The SSPD is maintained at a temperature  $T$  well below the critical temperature  $T_c$  (usually below  $T_c/2$ ) and carrying bias current  $I_b$  close to its critical current  $I_c$ . Such strip is essentially a 2D structure, as at the operation temperature

both the coherence length  $\xi$  and thermal length  $l_{th}$  are larger than film thickness  $d$  but smaller than the strip width  $w$ . The single-photon detection mechanism is based on the local hotspot (normal region) formation in the presence of bias current close to the strip critical current [3].

At wavelength  $\lambda \leq 1.3 \mu\text{m}$  quantum efficiency ( $QE$ ) of our best devices approaches 30% at 2 K with 35 ps timing jitter. Simultaneously, at 2 K the SSPD has negligibly low dark counts of  $2 \times 10^{-4} \text{ s}^{-1}$ . It provides NEP value of  $10^{-20} \text{ W/Hz}^{1/2}$  at  $\lambda \leq 1.3 \mu\text{m}$ .

We present here a new break-through in the SSPD technology: in a strive to improve the SSPD sensitivity in the middle infrared we fabricated SSPDs with the strip width reduced down to 50 nm (fig. 4 left). Such a narrow strip has critical current of a few  $\mu\text{A}$  thus providing a response voltage pulse that can hardly be resolved above the thermal noise level of the read-out electronics. To resolve this problem we connected 50-nm-wide and 10- $\mu\text{m}$ -long strips in parallel covering again the area of  $10 \mu\text{m} \times 10 \mu\text{m}$ . Being biased with a near critical current this device utilizes cascade switching mechanism [4]: absorption of a photon breaks the superconductivity in a strip leading to the bias current redistribution between other strips followed by their cascade switching. As the total current of all the strips is about 1 mA by the order of magnitude the response voltage of such an SSPD is several times higher compared to the traditional meander-shaped SSPDs.

Fig. 4 (right) presents quantum efficiency of standard meander-shaped SSPD (squares) and parallel-strip SSPD (triangles) vs wavelength in range from  $1.2 \mu\text{m}$  to  $4 \mu\text{m}$  measured at 5 K and 3 K temperatures. Hence it was difficult to determine the number of photons falling on the SSPD we present quantum efficiency in arbitrary units. One can see that at  $4 \mu\text{m}$  wavelength parallel-strip SSPD exhibits more than an order of magnitude higher quantum efficiency compared to the meander-shaped SSPD.

Because of the favorable characteristics and the possibility to be effectively coupled to single-mode optical fiber [5],[6] many applications of the SSPD have already been reported. The most impressive one is the report on the quantum key distribution (QKD) over 200 km [7] and 250 km [8] distance. The implementation of the SSPD for the research into emission of single-photon sources, e.g. quantum dots

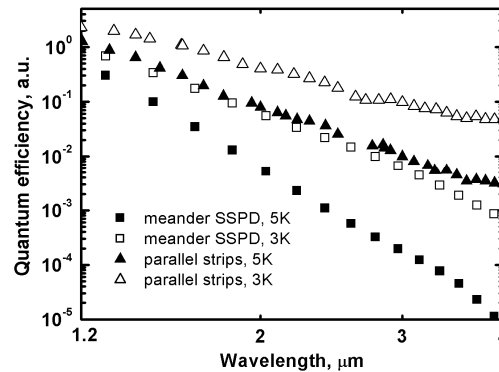
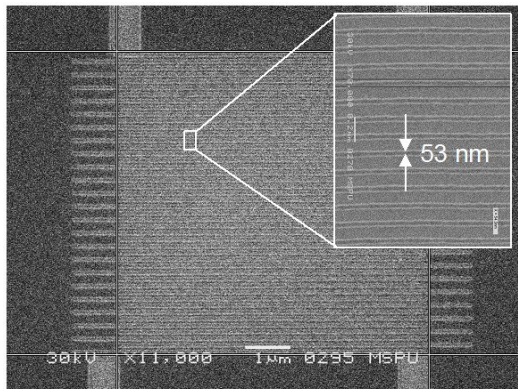


Fig. 4. SEM image of parallel-strip SSPD (left) with the strip width of 50 nm, and quantum efficiency in arbitrary units vs wavelength measured for standard meander-shaped SSPD (squares) and parallel-strip SSPD (triangles) at 5 K and 3 K temperatures (right)

or quantum wells, by time-correlated single-photon counting methods were reported as well [6], [9]-[11] where SSPD exhibits a better timing resolution (jitter) than avalanche photodiodes (APD) [12]. Recently we have successfully developed and implemented a photon-number resolving SSPD which demonstrated reliable resolution of up to 4 simultaneously absorbed photons [13].

THz direct detectors and HEB mixers are used in a wide range of application ranging from THz imaging for security (observation of hidden drugs, explosives and weapon) and medicine (THz probing of human tissues) to radioastronomy observation of stellar formation and dark matter (space observatories Herschel and Millimetron). SSPD due to their high quantum efficiency and picosecond timing resolution has already been successfully applied for study of quantum dot luminescence and for quantum key distribution (recent result is 250-km-long distance).

## References

1. G. Gol'tsman, O. Okunev, G. Chulkova, et al. Picosecond superconducting single-photon optical detector // Appl. Phys. Lett. 2001. V 79, P. 705-707.
2. G. N. Gol'tsman, K. Smirnov, P. Kouminov, et al. Fabrication of Nanostructured Superconducting Single-Photon Detectors // IEEE

Trans. Appl. Supercond., 2003. V. 13. P 192-195.

3. A. Semenov, G. Gol'tsman, A. Korneev Quantum detection by current carrying superconducting film // Physica C, 2001. V. 352. P. 349-356.

4. M. Ejrnaes, R. Cristiano, O. Quaranta, et al. A cascade switching superconducting single photon detector // Appl. Phys. Lett. 2007. V. 91. P. 262509.

5. W. Slysz, M. Wegrzecki, J. Bar, et al Fiber-coupled single-photon detectors based on NbN superconducting nanostructures for practical quantum cryptography and photon-correlation studies // Appl. Phys. Lett. 2006. V. 88. P. 261113.

6. C. Zinoni, B. Alloing, L. H. Li, et al Single-photon experiments at telecommunication wavelengths using nanowire superconducting detectors // Appl. Phys. Lett., 2007. V. 91. P. 031106.

7. Hiroki Takesue, Sae Woo Nam, Qiang Zhang, et al. Quantum key distribution over a 40-dB channel loss using superconducting single-photon detectors // Nat. Photon., 2007. V. 1. P. 343-348.

8. D. Stucki, N. Walenta, F. Vannel, et al. High rate, long-distance quantum key distribution over 250 km of ultra low loss fibres // New Journal of Physics 2009. V. 11. P. 075003.

9. M. Stevens, R. Hadfield, R. Schwall, et al. Fast lifetime measurements of infrared emitters using a low-jitter superconducting single-

photon detector // *Appl. Phys. Lett.*, 2006. V. 89. P. 031109.

10. *M. Stevens, R. Hadfeld, R. Schwall, et al.* Quantum dot single photon sources studied with superconducting single photon detectors // *Sel. Top. Quant. Electron, IEEE J.* 2006. V. 12. P. 1255.

11. *Korneev, A.; Vachtomin, Y.; Minaeva, O.; et al.* Single-Photon Detection System for Quantum Optics Applications // *Sel. Top. Quant. Electron., IEEE J.* 2007. V. 13. P. 944 – 951.

12. *T. Seki, H. Shibata, H. Takesue, et al.* Comparison of timing jitter between NbN superconducting single-photon detector and avalanche photodiode // *Physica C*, doi: 10.1016/j.physc.2010.05.156.

13. *A. Divochiy, F. Marsili, D. Bitauld, et al.* Superconducting nanowire photon number resolving detector at telecom wavelength // *Nat. Photon.*, 2008. V. 2, P. 302–306.

15.09.2010